Original Article

A cuproptosis-related long non-coding RNA signature to predict the prognosis and immune microenvironment characterization for lung adenocarcinoma

Shouzheng Ma[1#], Jun Zhu[2#], Mengmeng Wang[3#], Jianfei Zhu[1], Wenchen Wang[1], Yanlu Xiong[1], Runmin Jiang[1], Nagarashee Seetharamu[4], Fernando Conrado Abrão[5], Vinayaga Moorthi Puthamohan[6], Lei Liu[7,8], Tao Jiang[1]

[1]Department of Thoracic Surgery, Tangdu Hospital, Air Force Medical University (Fourth Military Medical University), Xi'an, China; [2]Department of General Surgery, The Southern Theater Air Force Hospital, Guangzhou, China; [3]Department of Drug and Equipment, Lintong Rehabilitation and Convalescent Centre, Xi'an, China; [4]Division of Medical Oncology and Hematology, Northwell Health Cancer Institute, Donald and Barbara Zucker School of Medicine at Hofstra/Northwell, Lake Success, NY, USA; [5]Hospital Alemão Oswaldo Cruz, Sao Paulo, Brazil; [6]Department of Human Genetics and Molecular Biology, Bharathiar University, Coimbatore, Tamil Nadu, India; [7]Department of Gastroenterology, Tangdu Hospital, Air Force Medical University (Fourth Military Medical University), Xi'an, China; [8]Department of Gastroenterology, Daping Hospital, Army Medical University, Chongqing, China

Contributions: (I) Conception and design: S Ma, Jun Zhu; (II) Administrative support: T Jiang, L Liu; (III) Provision of study materials or patients: T Jiang, L Liu; (IV) Collection and assembly of data: Jianfei Zhu, W Wang, Y Xiong, R Jiang; (V) Data analysis and interpretation: S Ma, Jun Zhu, M Wang; (VI) Manuscript writing: All authors; (VII) Final approval of manuscript: All authors.

[#]These authors contributed equally to this work and should be considered as co-first authors.

Correspondence to: Tao Jiang. Department of Thoracic Surgery, Tangdu Hospital, Air Force Medical University (Fourth Military Medical University), 569 Xinsi Road, Xi'an 710038, China. Email: Jiangtaochest@163.com; Lei Liu. Department of Gastroenterology, Tangdu Hospital, Air Force Medical University (Fourth Military Medical University), 569 Xinsi Road, Xi'an 710038, China. Email: liulei84207@163.com.

Background: Cuproptosis or copper-dependent cell death is a newly identified non-apoptotic cell death pathway which plays a critical role in the development of multiple cancers. Long non-coding RNAs (lncRNAs) are increasingly recognized as crucial regulators of programmed cell death and lung adenocarcinoma (LUAD) development, and a comprehensive understanding of cuproptosis-related lncRNAs may improve prognosis prediction of LUAD. However, few studies have explored the association of cuproptosis-related lncRNAs with the prognosis of LUAD.

Methods: The RNA sequencing data and corresponding clinical information of patients were extracted from The Cancer Genome Atlas (TCGA) database. Five hundred LUAD patients were randomly divided into a training (n=250) and a testing cohort (n=250). Pearson correlations were performed to identify cuproptosis-related lncRNAs, and univariate Cox regression was performed to screen prognostic lncRNAs. A cuproptosis-related lncRNAs prognostic signature (CLPS) was constructed by the least absolute shrinkage and selection operator Cox regression. Kaplan-Meier analysis, receiver operating characteristic curves, and multivariate Cox regression were performed to verify the prognostic performance of CLPS. Additionally, immune cell infiltration was estimated using the single-sample gene-set enrichment analysis. pRRophetic algorithm and Tumor Immune Dysfunction and Exclusion algorithm were used to assess the immunotherapy and chemotherapy response, respectively.

Results: CLPS was established based on 61 cuproptosis-related prognostic lncRNAs and exhibited a satisfactory performance predicting LUAD patients' survival (area under the curve at 1, 3, 5 years was 0.784, 0.749, 0.775, respectively). multivariate Cox analysis confirmed the independent prognostic effect of CLPS (hazard ratio: 1.128; 95% confidence interval: 1.071–1.189; P<0.001), and a nomogram containing it exhibited robust validity in prognostic prediction. We further demonstrated a higher CLPS-risk score was associated with lower levels of signatures including immune cell infiltration, immune activation, and immune checkpoints.

Conclusions: The CLPS serves as an effective predictor for the prognosis and therapeutic responses of LUAD patients. Our findings provide promising novel biomarkers and therapeutic targets for LUAD.

Keywords: Lung adenocarcinoma (LUAD); cuproptosis; long non-coding RNAs (lncRNAs); prognostic signature; tumor microenvironment (TME)

Submitted Jun 16, 2022. Accepted for publication Sep 28, 2022.
doi: 10.21037/tlcr-22-660
View this article at: https://dx.doi.org/10.21037/tlcr-22-660

Introduction

Lung cancer is the leading cause of cancer-related mortality and the second most common cancer worldwide (1). Lung adenocarcinoma (LUAD) is the most prevalent histologic sub-type and accounts for 40–50% of lung cancer (2). Despite the great success of molecular targeted therapy and immunotherapy in cancer treatment, as well as increasingly abundant prediction models, both diagnostic and prognostic, the prognosis for LAUD remains poor due to the heterogeneity of tumors and complexity of molecular mechanisms (3,4). Indeed, it is estimated that the 5-year survival rates vary from 4–17% depending on stage differences (5). Therefore, there is a continued need to develop novel sensitive and effective biomarkers for prognosis prediction and providing individualized therapy for LUAD.

Cuproptosis is a novel form of programmed cell death (PCD) distinguished from others, such as apoptosis, necrosis, pyroptosis, and ferroptosis (6,7). As a copper-induced cell death, cuproptosis is characterized by intracellular copper accumulation-triggered aggregation of mitochondrial lipoylated proteins [lipoylated dihydrolipoamide S-acetyltransferase (DLAT)] and the instability of Fe-S proteins, resulting in proteotoxic stress (8). The induction of PCD has been known to be a reliable approach for cancer therapy (9-11), making cuproptosis a novel promising strategy to inhibit tumor progression by triggering tumor cell death (7). However, the specific mechanisms of cuproptosis underlying the tumorigenesis, progression, and tumor microenvironment (TME) remodeling remain unclear.

With the rapid development of high throughput sequencing, long non-coding RNAs (lncRNAs) have become a major focus of PCD (12,13), which plays a critical role in the development of multiple cancers including LUAD (14,15). LncRNAs participate in complex biological processes by interacting with DNA, RNA, and proteins. Cumulative evidence has demonstrated that the dysregulation of lncRNAs in LUAD is widely involved in tumor cell proliferation, invasion, and metastasis, as well as shaping the TME (16-18). Studying cuproptosis-related lncRNAs may provide further insight into the role of this pathway in cancer, potentially serve as prognostic/predictive biomarker and help identify novel therapeutic targets for LUAD. This formed the basis of our Cancer Genome Atlas (TCGA)-based investigation, where we mined potential cuproptosis-related lncRNAs based on a TCGA-LUAD cohort to construct a cuproptosis-related lncRNAs prognostic signature (CLPS). We also explored the mechanism of cuproptosis-related lncRNAs in tumor progression and the TME heterogeneity through functional analysis and immune infiltration analysis. Additionally, we assessed the potential role of CLPS in predicting therapeutic response to cytotoxic chemotherapy and immunotherapy. We present the following article in accordance with the TRIPOD reporting checklist (available at https://tlcr.amegroups.com/article/view/10.21037/tlcr-22-660/rc).

Methods

Data extraction and preprocessing

The design and implementation of this study are shown in detail in *Figure 1*. The RNA sequencing data and corresponding clinical information of 522 LUAD patients were extracted from TCGA database. Twenty-two patients were excluded due to the lack of available survival information, and 500 patients with corresponding clinicopathological information were eventually included for further analysis. These patients were randomly divided (conservative random 1:1 split) into a training (n=250) and a testing cohort (n=250) at a 1:1 ratio using the "caret" R package (19). The somatic mutation profiles of LUAD samples were downloaded from TCGA database. The

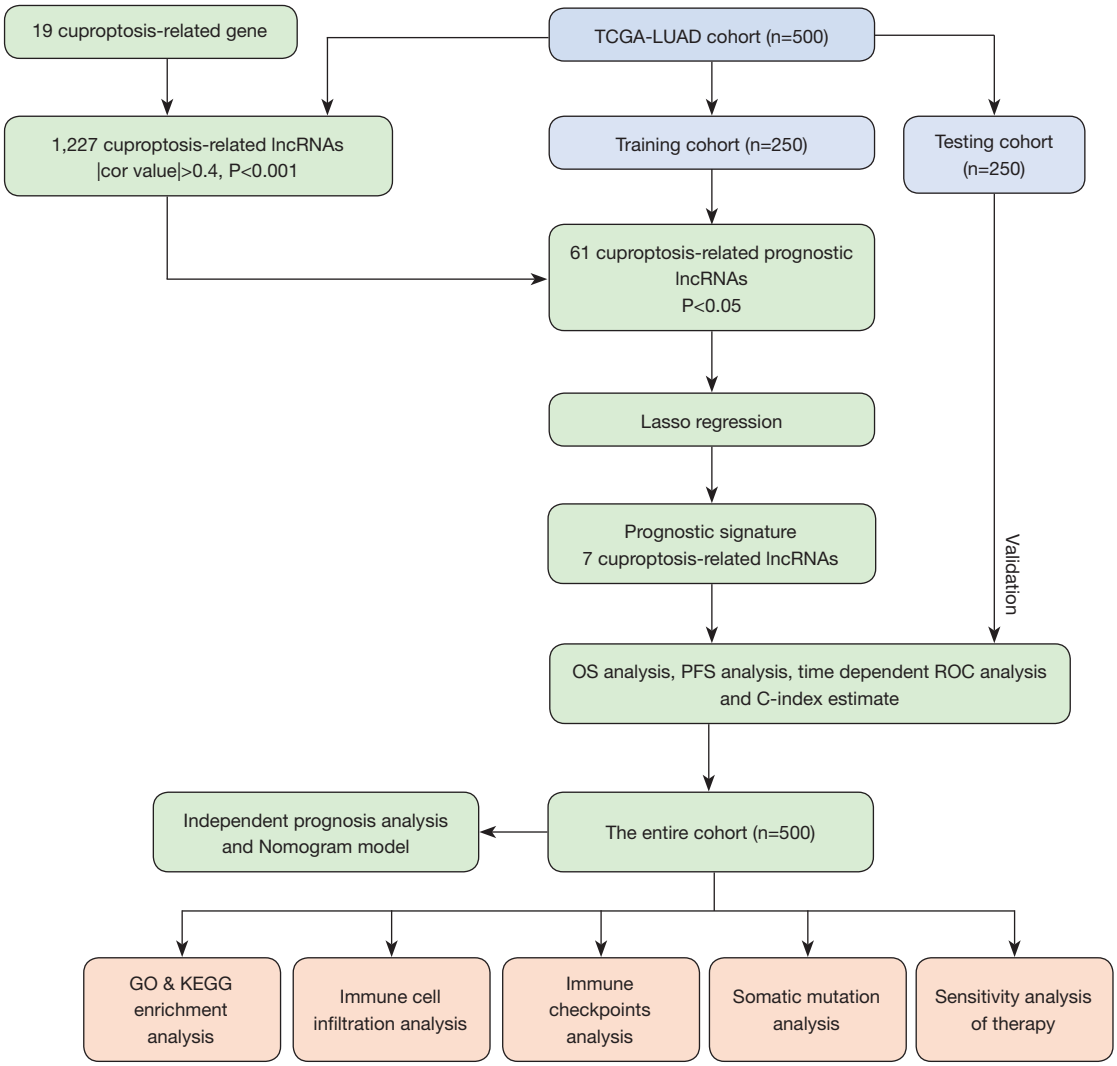

Figure 1 Overview of the study design and analytical flow. TCGA, The Cancer Genome Atlas; LUAD, lung adenocarcinoma; lncRNAs, long non-coding RNAs; LASSO, least absolute shrinkage and selection operator; OS, overall survival; PFS, progression-free survival; ROC, receiver operator characteristic; GO, Gene Ontology; KEGG, Kyoto Encyclopedia of Genes and Genomes.

study was conducted in accordance with the Declaration of Helsinki (as revised in 2013).

Identification of cuproptosis-related lncRNAs

We retrieved 19 cuproptosis-related genes from previous studies (6-8,20) as shown in Table S1. The mRNA and lncRNA expression profiles were classified, and Pearson correlation analysis was then performed to reveal the correlation between the expression of cuproptosis-related genes and corresponding lncRNAs. A total of 1,227 cuproptosis-related lncRNAs were identified based on the standard that the P value <0.001 and the absolute value of Pearson correlation coefficient >0.4.

Construction and validation of the CLPS

In the training cohort, univariate analyses for overall survival (OS) were performed using a Cox proportional hazards regression model to screen cuproptosis-related prognostic lncRNAs with a P value filter of <0.05. A least absolute shrinkage and selection operator (LASSO) Cox regression (21) was then conducted using the "glmnet" R package to identify the robust prognostic lncRNAs and fitted a multivariable Cox

regression model. Finally, a CLPS including seven lncRNAs was constructed: $\text{Risk score} = \sum_i^n \alpha i \times \beta i$, where αi means the coefficients, and βi represents the expression value of each cuproptosis-related lncRNAs.

The median risk score from the training cohort was used as the cut-off point to define CLPS-based high-risk or low-risk scores. Kaplan-Meier curves were performed to estimate OS and progression-free survival (PFS) through the "survival" and "survminer" R package, and log-rank tests were used to compare the curves. Time-dependent receiver operating characteristic (ROC) analyses and the area under the curve (AUC) calculation were performed using the "timeROC" R package to evaluate the predictive capacity of the CLPS. The Harrell's concordance index (C-index) was calculated using the "survival" R package to quantify the performance of CLPS, and the Principal Components Analysis (PCA) was performed and visualized with the "scatterplot3d" R package. The same analyses were performed on the testing cohort for validation.

Independent prognostic analysis and nomogram construction

To confirm whether the CLPS was independent of other clinical characteristics in predicting the OS of LUAD patients, univariate and multivariate analyses were performed with a Cox proportional hazards regression model which included the CLPS and several clinical characteristics. Further, a novel nomogram which included age, gender, stage, and the CLPS was established to predict patient survival.

Functional enrichment analysis

Differentially expressed genes (DEGs) between the high and low-risk groups were identified with a significance threshold of $|\log_2 FC| > 1$ and false discovery rate (FDR) <0.05 using the "limma" R package. To explore the difference in biological pathways between the two groups, the "clusterProfiler" R package was used to perform Gene Ontology (GO) and Kyoto Encyclopedia of Genes and Genomes (KEGG) enrichment analyses for these DEGs. Significant enrichment pathways (P value <0.05) are displayed in the bar plot and bubble plot.

Analysis of the TME characterization

The Estimation of Stromal and Immune cells in Malignant Tumor tissues using Expression data (ESTIMATE) algorithm (22) was conducted to infer the fraction of stromal and immune cells (defined as the stromal and immune scores) in each sample using the "ESTIMATE" R package (v1.1.0, https://bioinformatics.mdanderson.org/estimate/rpackage.html). The ESTIMATE score is a composite score summarizing the immune score and the stromal score, while the tumor purity, defined as the percentage of malignant cells in a solid tumor, is inversely proportional to the ESTIMATE score. The single-sample gene-set enrichment analysis (ssGSEA) algorithm (23) was conducted to estimate the immune cell infiltration, implemented in the "GSVA" R package, and 29 immune signature-specific gene sets were referred to the published literature (24,25). The gene sets of immune activation and immune-checkpoints were derived from Mariathasan *et al.* (26,27).

Prediction of response to immunotherapy and chemotherapy

We further investigated whether the CLPS could predict the clinical response to immunotherapy and chemotherapy. The gene signatures of T cell dysfunction and prediction of cancer immunotherapy response on cancer was inferred by Tumor Immune Dysfunction and Exclusion (TIDE, http://tide.dfci.harvard.edu/), a novel but effective algorithm as Jiang *et al.* described (28). Generally, a higher TIDE score predicts a poor response to immunotherapy. The pRRophetic algorithm was used to estimate the 50% inhibiting concentration (IC_{50}) values of five common first-line chemotherapy drugs (including cisplatin, paclitaxel, etoposide, gemcitabine, and doxorubicin) for LUAD (29).

Statistical analysis

All statistical analyses were performed using R software (version 4.1.1) and attached packages. Wilcox test was used to assess the differences between the high and low-risk groups, and Pearson correlation analysis was used to determine the correlation coefficient. Survival curves were performed using the Kaplan-Meier method, and the log-rank test was used to determine the statistical significance of differences. The waterfall plots of the mutational landscape were generated using the "maftools" R package (30). All reported P values were two-tailed, and statistically significant was defined as P value <0.05.

Results

Construction and validation of the CLPS

The 500 LUAD patients were randomly divided into a training (n=250) and a testing cohort (n=250), and no statistically significant difference was detected in clinical characteristics between the two (Table S2). Based on the identified 1,227 cuproptosis-related lncRNAs (available online: https://cdn.amegroups.cn/static/public/TLCR-22-660-1.xlsx, Figure S1), 61 cuproptosis-related prognostic lncRNAs (*Figure 2A*) were screened by univariate analysis in the training cohort, and a LASSO Cox regression analysis was performed based on them (*Figure 2B*,*2C*). Finally, seven lncRNAs were adopted to constitute the CLPS (Table S3, *Figure 2D*). Risk scores of patients in the training cohort and the testing cohort were calculated, respectively (Tables S4,S5), and there were significant correlations between the cuproptosis-related gene expressions and the expressions of the seven CLPS-lncRNAs (*Figure 2E*). As shown in Figure S1B-S1E, PCA based on the seven CLPS-lncRNAs exhibited an absolute distribution difference of patients from the two groups.

Kaplan-Meier survival curves indicated patients with lower risk scores showed significantly better OS and PFS in both training (*Figure 3A*,*3B*) testing cohorts (*Figure 3C*,*3D*). As shown in *Figure 3E*,*3F*, the AUC) of the risk score reached 0.784 at 1 year, 0.749 at 3 years, and 0.775 at 5 years in the training cohort, and were still greater than 0.6 in the testing cohort. C-index values further indicated the good prediction accuracy of the CLPS (*Figure 3G*,*3H*). As shown in *Figure 3I*,*3J*, high-risk patients exhibited a higher probability of death than low-risk patients, and the heatmaps suggested AC090541.1 (a human DNA sequence from clone RP11-1105O14 on chromosome 8) and AC107021.2 (a human DNA sequence from clone RP11-274H2 on chromosome 3) were upregulated in the high-risk group, while LINC02390 (long intergenic non protein coding RNA 2390), NIFK-AS1 (NIFK antisense RNA 1), AC026355.2 (a human DNA sequence from clone RP11-114M1 on chromosome 3), MIR34AHG (MIR34A host gene), and LINC01215 (long intergenic non protein coding RNA 1215) were downregulated in the high-risk group. The above analysis performed in the entire LUAD cohort also showed consistent results (Figure S2A-S2E). Additionally, subsequent subgroup survival analyses (Figure S2F-S2K) demonstrated the prognostic value of the CLPS remained statistically significant for each subgroup based on gender (male, female), age (≤65, >65 years), and clinical stage (I–II, III–IV).

Analysis of clinical characteristics and construction of the nomogram

We next performed a series of analyses based on clinical characteristics, and ROC analysis suggested the CLPS had a stronger prognostic capacity than other clinical characteristics (*Figure 4A*). Univariate (*Figure 4B*) and multivariate (*Figure 4C*) Cox analyses confirmed the CLPS as an independent prognostic factor for predicting patient outcomes [HR: 1.128 (1.071–1.189), P<0.001]. Furthermore, a nomogram consisting of age, gender, clinical stage, and CLPS was constructed (*Figure 4D*) as a visualizing prognostic tool to quantify the survival probabilities at 1, 3, and 5 years. Calibration curves indicated that the observed and predicted survival proportions at 1, 3, and 5 years exhibited good concordance in the LUAD cohort (*Figure 4E*).

Functional enrichment analyses

A total of 224 DEGS were identified between the high and low-risk groups (Table S6). To reveal the biological pathways associated with the CLPS, GO functional enrichment and KEGG pathway enrichment analyses were performed based on the DEGs between the high and low-risk groups. As expected, GO analysis suggested the DEGs were primarily enriched in pathways related to immune cell-infiltrating (e.g., lymphocyte, leukocyte, macrophage and mononuclear cell proliferation, and myeloid leukocyte migration), immune activation (e.g., antimicrobial humoral response, humoral immune response), extracellular matrix (ECM) remodeling (e.g., collagen-containing ECM, ECM structural constituent), and cytokine-cytokine receptor interactions (*Figure 5A*,*5B*). Similarly, KEGG analysis revealed DEGs were mainly focused on critical pathways involved in cytokine signaling (cytokine-cytokine receptor interaction, chemokine signaling pathway), ECM remodeling (focal adhesion, ECM-receptor interaction), and immune-related pathways (primary immunodeficiency, B cell receptor signaling pathway) (Figure S3A,S3B).

TME characterization

The ESTIMATE analysis results indicated tumors with lower CLPS-risk scores were remarkably abundant in immune cells, while no significant difference in stromal cell abundance was observed in the two groups (*Figure 6A-6D*).

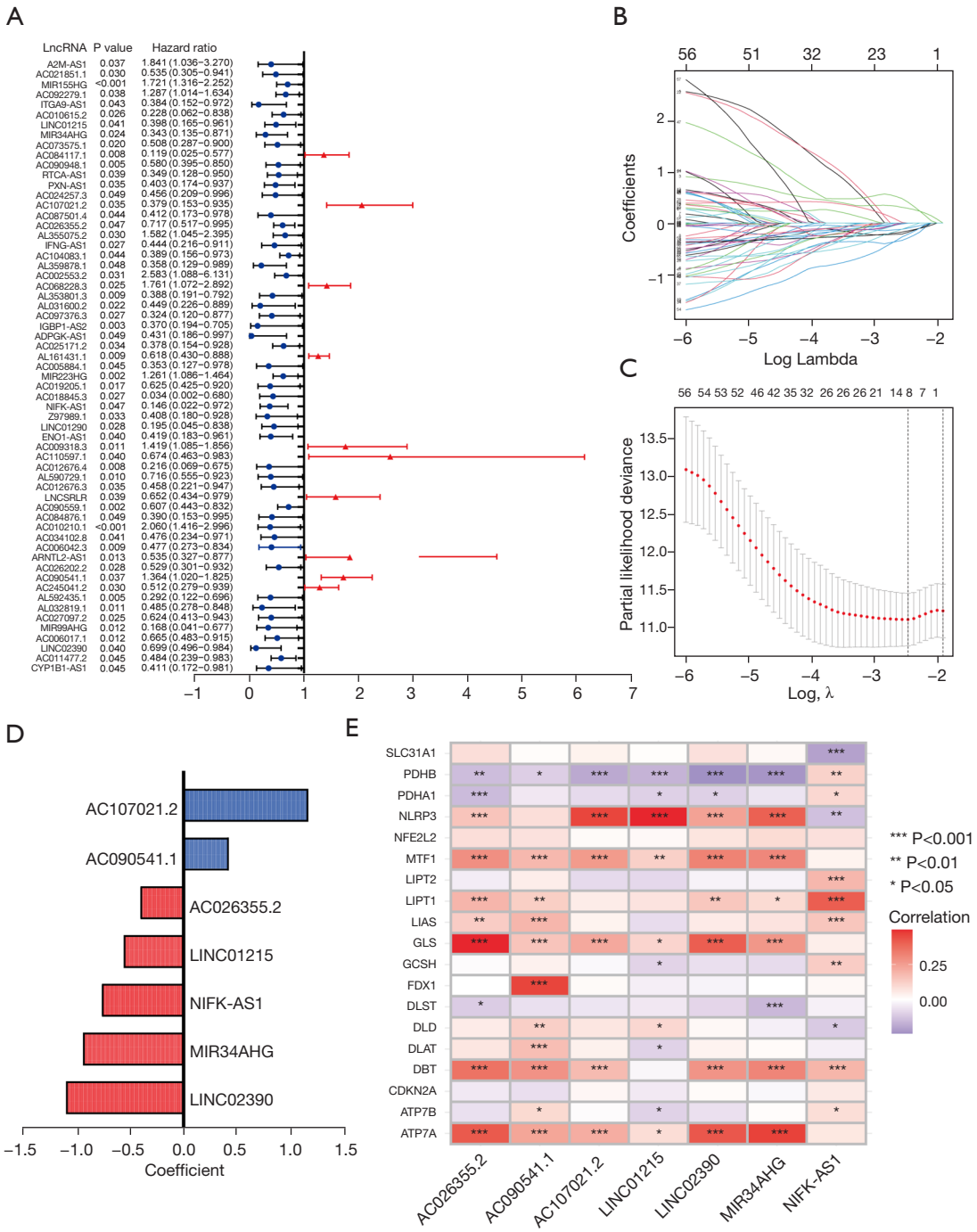

Figure 2 Construction of a CLPS. (A) Univariate Cox regression analysis for 61 cuproptosis-related prognostic lncRNAs. (B,C) LASSO Cox regression analysis based on 61 cuproptosis-related prognostic lncRNAs. (D) Coefficients of the LASSO Cox model with the minimum lambda criteria. (E) Correlation analyses of cuproptosis-related genes and the CLPS lncRNAs. CLPS, cuproptosis-related lncRNAs prognostic signature; lncRNAs, long non-coding RNAs; LASSO, least absolute shrinkage and selection operator.

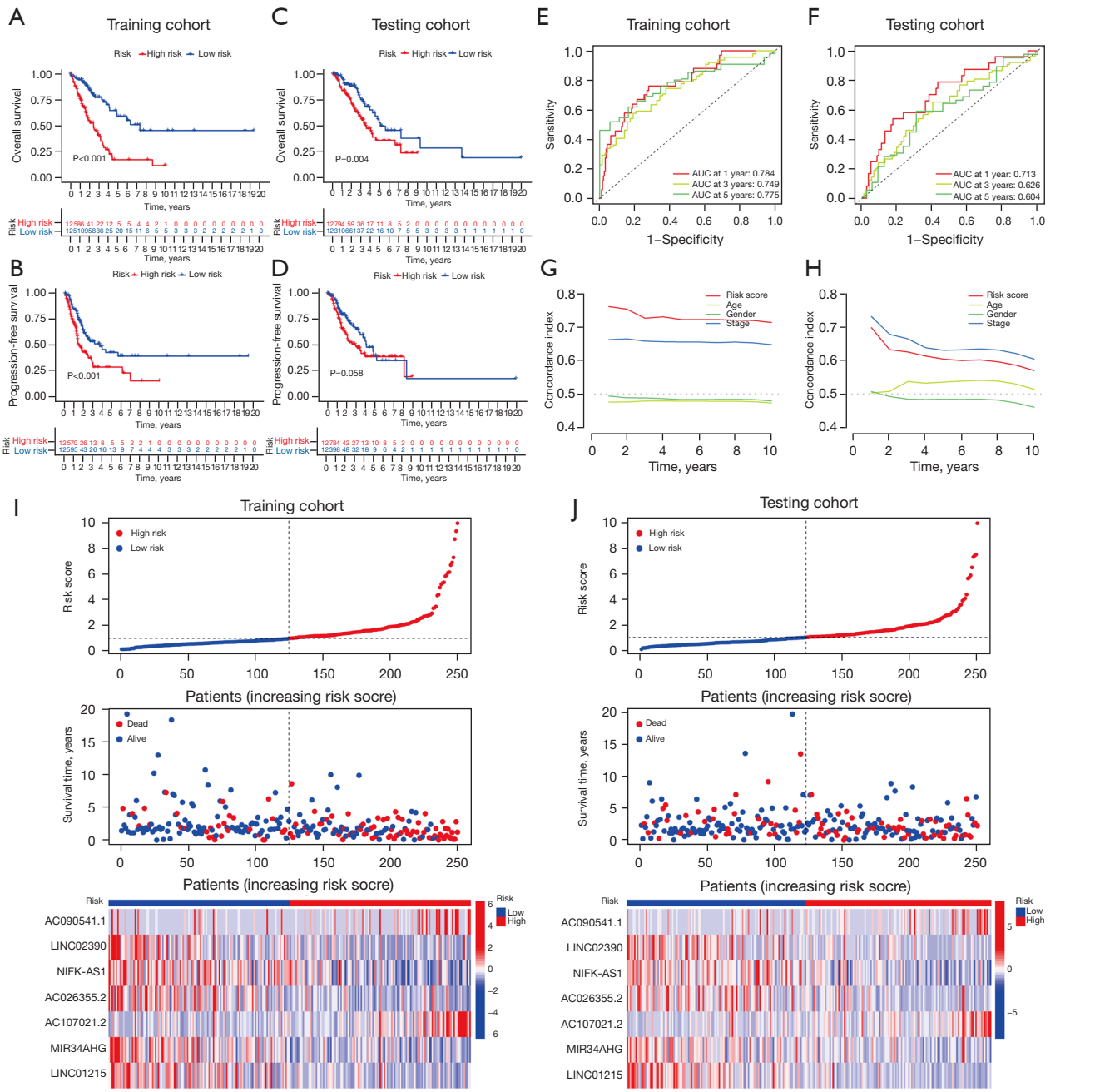

Figure 3 Survival analysis and validation of the CLPS in LUAD patients. (A,B) Kaplan-Meier curves of (A) OS and (B) PFS in the training cohort. (C,D) Kaplan-Meier curves of (C) OS and (D) PFS in the testing cohort. (E,F) ROC curves for the CLPS risk score at 1, 3, and 5 years in (E) training cohort and (F) testing cohort. (G,H) The C-index of the CLPS risk score and other clinical characteristics in (G) the training cohort and (H) testing cohort. (I,J) Survival state (the middle section) of the patients sorted according to the risk scores (the top section) and the differences in the CLPS lncRNAs between high-risk and low-risk groups (the bottom section) in (I) the training cohort and (J) testing cohort. AUC, area under the curve; CLPS, cuproptosis-related lncRNAs prognostic signature; LUAD, lung adenocarcinoma; OS, overall survival; PFS, progression-free survival; ROC, receiver operating characteristic; lncRNAs, long non-coding RNAs.

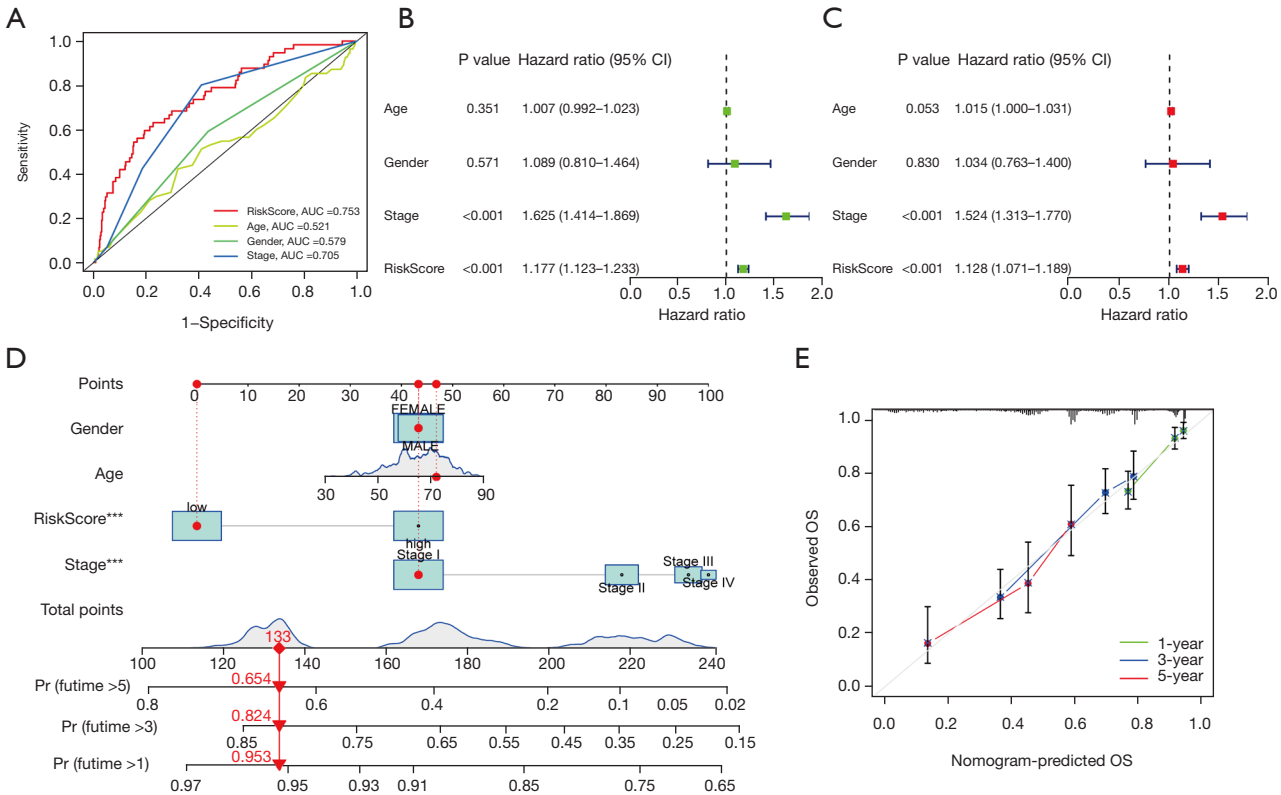

Figure 4 Establishment of a novel nomogram for predicting prognosis of LUAD patients. (A) ROC curve for the risk signature and several clinical characteristics at 1-year in the entire cohort. (B) Univariate and (C) multivariate analyses for the risk score using the Cox regression model. (D) A nomogram for predicting OS of LUAD patients constructed based on the entire cohort. (E) The calibration curves of the nomogram predicted 1-, 3-, and 5-year OS in the entire cohort. ***, P<0.001. AUC, area under the curve; LUAD, lung adenocarcinoma; ROC, receiver operating characteristic; OS, overall survival.

In addition, the ssGSEA analysis demonstrated higher CLPS-risk scores were significantly associated with reduced levels of majority immune-related signatures (*Figure 6E*), including immune cell infiltration (e.g., dendritic cells, B cells, $CD8^+$ T cells, mast cells, neutrophils, T helper cells, and tumor infiltrating lymphocyte), immune activation (cytolytic activity, human leucocyte antigen, inflammation promoting, T cell co-stimulation, and type II interferon response), and immune checkpoints. Furthermore, we analyzed the expression of chemokines and cytokines considered to be relevant to immune activation and immune checkpoints, respectively, and as expected, the mRNAs related to immune activation were significantly downregulated in the high-risk group (*Figure 6F*). There were also negative correlations between the CLPS-risk scores and the expression of most immune checkpoint-related mRNAs (*Figure 6G*, *Figure S4A-S4I*). The above results revealed a non-negligible association of the CLPS with different TME immune landscapes, which might in turn affect tumor affect tumor progression and the therapeutic response.

Analysis of tumor somatic mutation and prediction of the therapeutic response

Accumulated evidence indicates the tumor mutational burden (TMB) is a predictive biomarker for response to immune checkpoint inhibitor therapy (31,32). We evaluated the intratumoral somatic mutation landscape to indirectly predict the immunotherapeutic outcomes. The waterfall plots suggested the high-risk group exhibited more extensive somatic mutation than the low-risk group (*Figure 7A*,*7B*), while subsequent Kaplan-Meier survival curves showed patients with higher TMB had better OS than lower TMB (*Figure 7C*). As shown in *Figure 7D*, combining the CLPS-risk score and TMB exhibited a

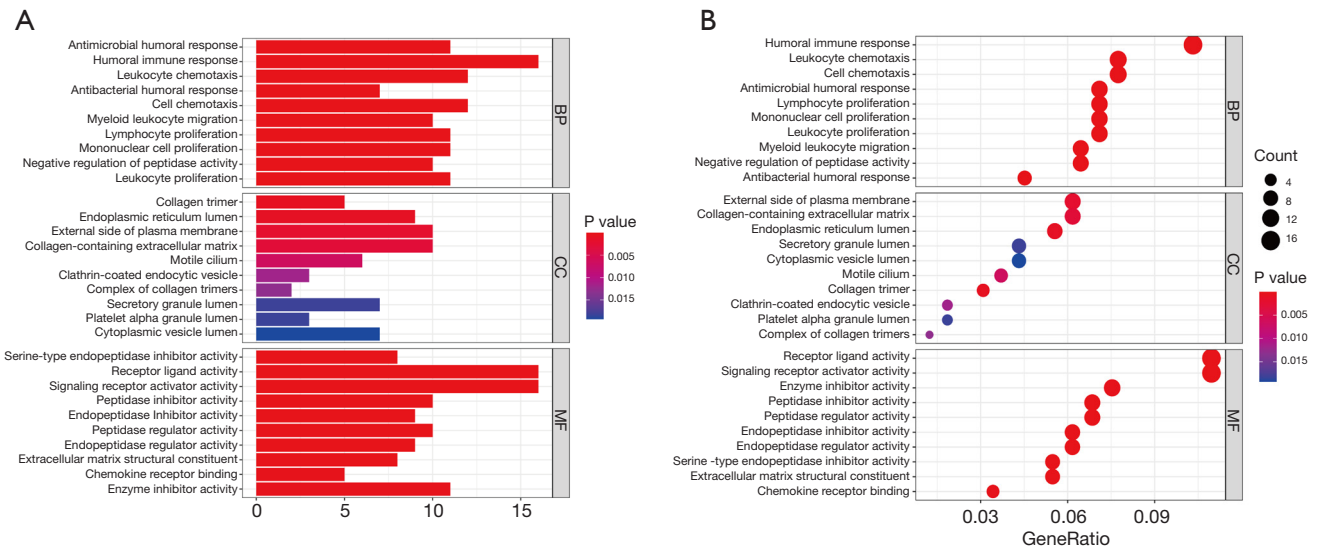

Figure 5 Functional annotation for DEGs between the high and low-risk groups using GO enrichment analysis. (A) The bar plot and (B) bubble plot showing the significantly enriched GO pathways. The bubble color representing the P value, and the bubble size representing the number of genes in the relevant pathway. BP, biological process; CC, cellular component; MF, molecular function; DEGs, differentially expressed genes; GO, Gene Ontology.

greater prognostic value for LUAD patients.

To directly predict the response to immunotherapy, we estimated the TIDE score of all LUAD patients based on the TIDE algorithm. As shown in *Figure 8A*, the high-risk group showed a significantly lower TIDE score compared with the low-risk group, which indicated a better response to immunotherapy in patients with higher CLPS-risk scores. Moreover, there were significant negative correlations of the CLPS-risk score with the IC_{50} to cisplatin (*Figure 8B,8C*), paclitaxel (*Figure 8D,8E*), etoposide (*Figure 8F,8G*), gemcitabine (*Figure 8H,8I*), and doxorubicin (*Figure 8J,8K*), which indicated patients with higher CLPS-risk scores had a better response to these chemotherapy agents.

Discussion

LUAD is considered a highly heterogeneous tumor, where multiple genetic, epigenetic, and phenotypic alterations drive its development and progression (33,34). With growing understanding of the molecular mechanisms of LUAD, there has been a rapid evolution of personalized therapies for treatment of LUAD such as epidermal growth factor receptor (EGFR) inhibitors and programmed cell death 1 (PD1)/programmed cell death ligand 1 (PD-L1) inhibitors (35,36). Unfortunately, primary and secondary resistance and variable responses to currently available treatments present an ongoing challenge, highlighting the need for continued exploration of novel molecular biomarkers for individualized prognosis and treatment of LUAD. Several studies have emphasized the critical importance of PCD in battling cancer, including apoptosis, necrosis, pyroptosis, and ferroptosis (10,37). Cuproptosis is a newly discovered form of PCD, which has been shown to have antitumor potential (7) but the underlying mechanisms have not been clearly identified. With the development of next-generation sequencing technology (38), an increasing number of lncRNAs have been identified and confirmed to play critical roles in initiation and progression of LUAD (16,17). We hypothesized that cuproptosis-related lncRNAs may have a great potential as diagnostic biomarkers and help identify therapeutic targets in LUAD.

To the best of our knowledge, this study is the first to comprehensively explore the prognostic significance of cuproptosis-related lncRNAs in LUAD. First, we identified 61 cuproptosis-related prognostic lncRNAs and constructed a CLPS based on seven lncRNAs, including five protective factors (LINC02390, MIR34AHG, NIFK-AS1, LINC01215, AC026355.2) and two risk factors (AC107021.2, AC090541.1). MIR34AHG is the host gene of miR-34a and may have biological functions similar to the miR-34 family, which inhibits the progression of LUAD

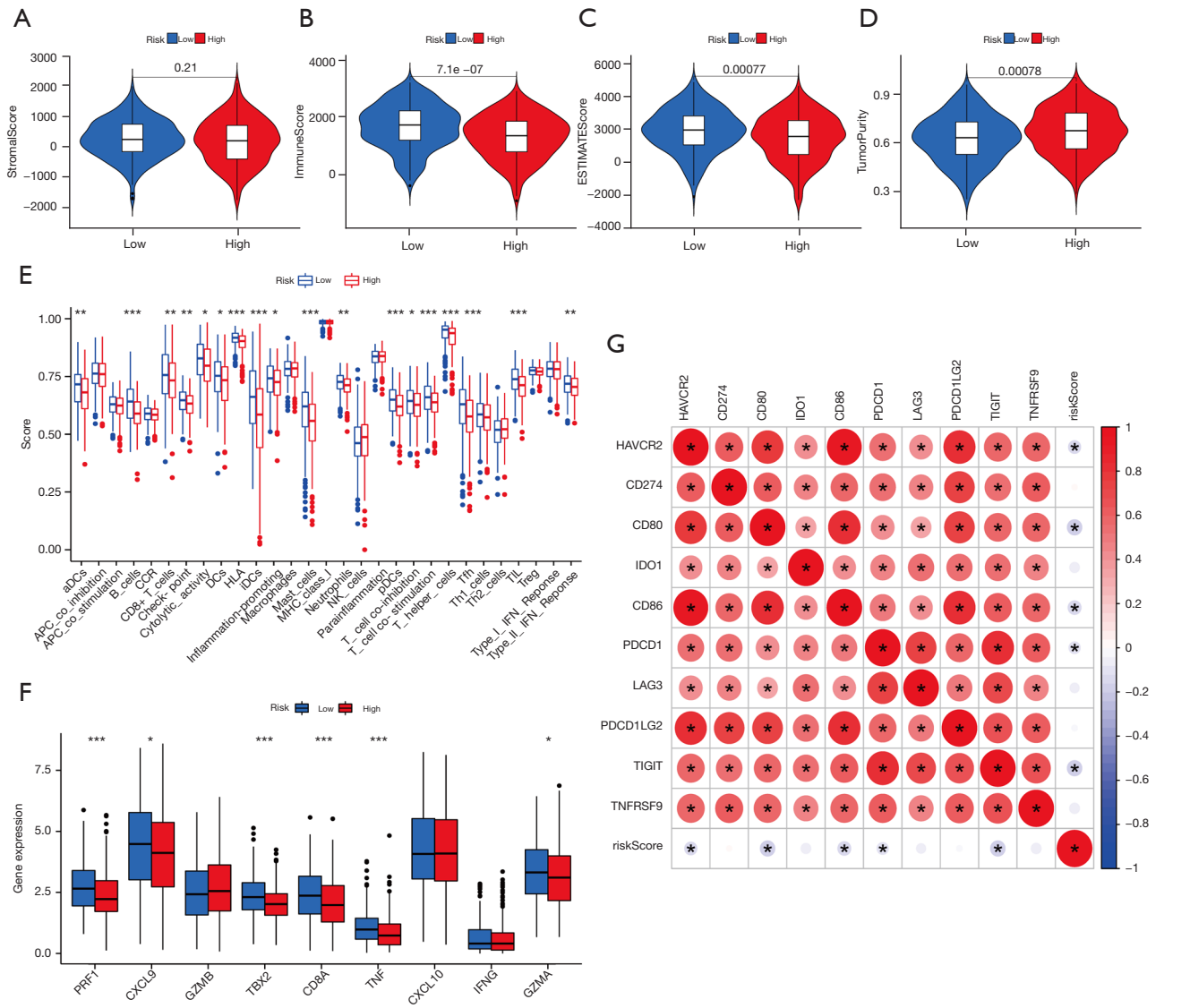

Figure 6 TME characteristics in the high- and low-risk groups. (A-D) Difference in the (A) stromal score, (B) immune score, (C) estimate score, and (D) tumor purity between the two groups. (E) Difference in the levels of 29 TME signatures between the two groups. (F) Difference in the immune-activation related gene expression between the two groups. The horizontal line indicates the median, the lower and upper boundaries of the boxes the interquartile range, and the dots the outliers. Asterisks indicate statistical significance, *, P<0.05; **, P<0.01; ***, P<0.001. (G) Correlations between the risk score and immune-checkpoint related gene expression. Positive correlation was marked with red and negative correlation with blue. The circle color represents Spearman coefficient value, the size of circle is inversely proportional to the P value, and the * stands for P<0.001. TME, tumor microenvironment.

(39,40). Importantly, the CLPS exhibited a satisfactory performance in predicting OS and PFS in LUAD, which provided an effective prognostic tool to complement traditional clinical indices. MIR34AHG, NIFK-AS1, LINC01215, and AC026355.2 have been confirmed to be associated with progression or prognosis of tumors. NIFK-AS1, LINC01215, AC026355.2 have also been previously shown to have a positive effect on prognosis (41-44). Expression of MIR34AHG, NIFK-AS1, and LINC01215 have also been associated with the heterogeneity of immune cell infiltration (41,42,45), suggesting that the CLPS may be beneficial in predicting survival outcomes as well as

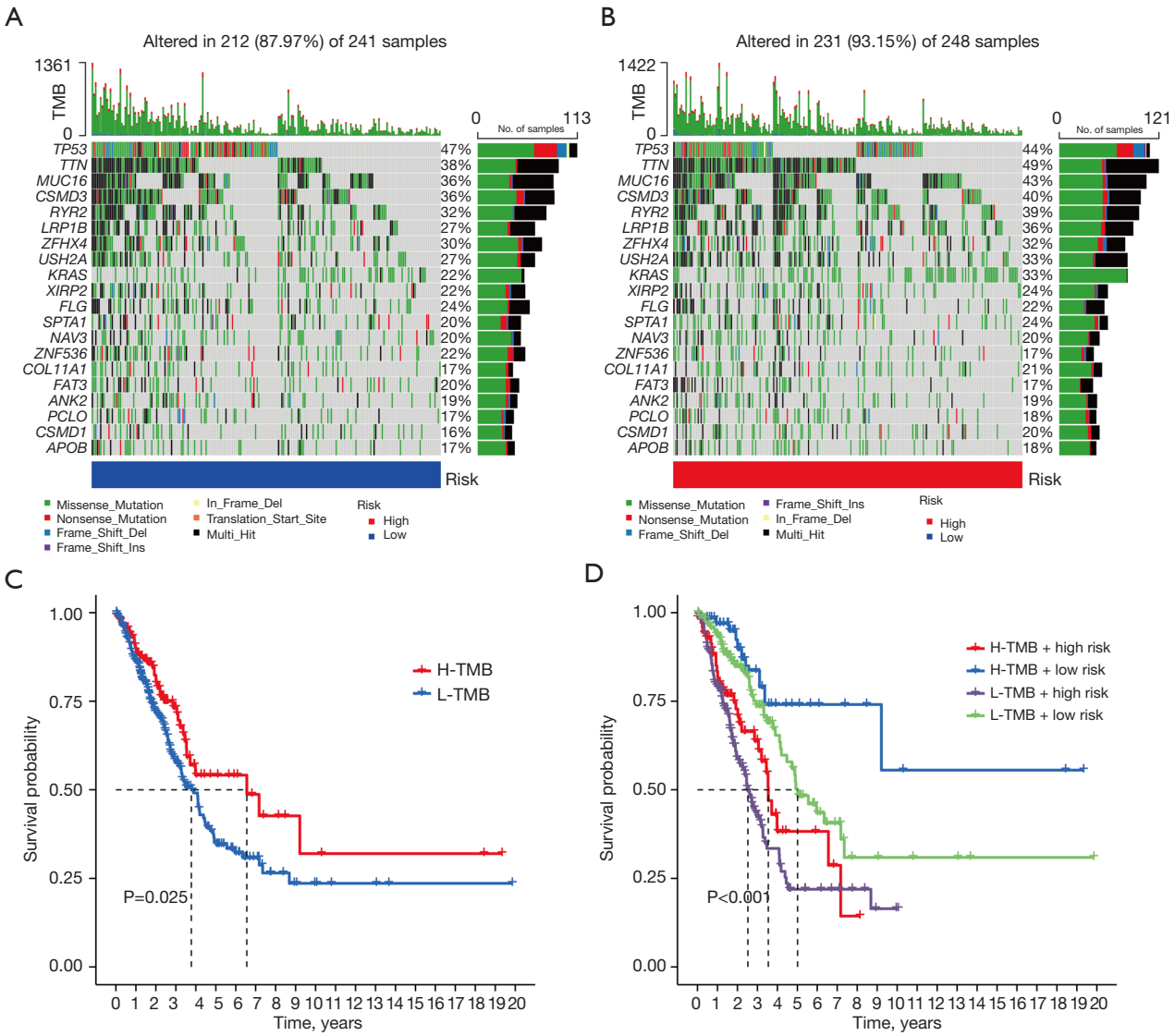

Figure 7 Analysis of tumor somatic mutation in LUAD patients with different risk scores. (A,B) The top barplot depicts TMB and mutation frequency in each gene is given on the right. The right barplot depicts the proportion of each variant type. The stacked barplot below depicts fraction of conversions in each sample. (C) Kaplan-Meier curve of OS for high and low-TMB groups. (D) Kaplan-Meier curve of OS for subgroup patients stratified by the risk score and TMB. TMB, tumor mutational burden; H, high; L, low; LUAD, lung adenocarcinoma; OS, overall survival.

assessing immune regulation in cancer.

Our CLPS exhibited a satisfactory performance in predicting OS and PFS in LUAD, providing an effective prognostic tool to complement traditional clinical indices. In addition, our analysis validated previously observed survival protective effect of MIR34AHG, NIFK-AS1, LINC01215, and AC026355 (41-44). Furthermore, our study demonstrated for the first time that three lncRNAs, namely LINC02390, AC107021.2, and AC090541.1 are prognostic in LUAD, with LINC02390 having a positive effect and the others a negative effect on prognosis. These findings warrant further exploration.

The TME plays a crucial role in tumorigenesis and development (46,47), and is an important determinant of prognosis and treatment response for LUAD patients (48,49). In particular, tumor infiltrating $CD8^+$ T cells, which are key to an effective anti - tumor response, and high $CD8^+$ T cell infiltration has been linked with favorable

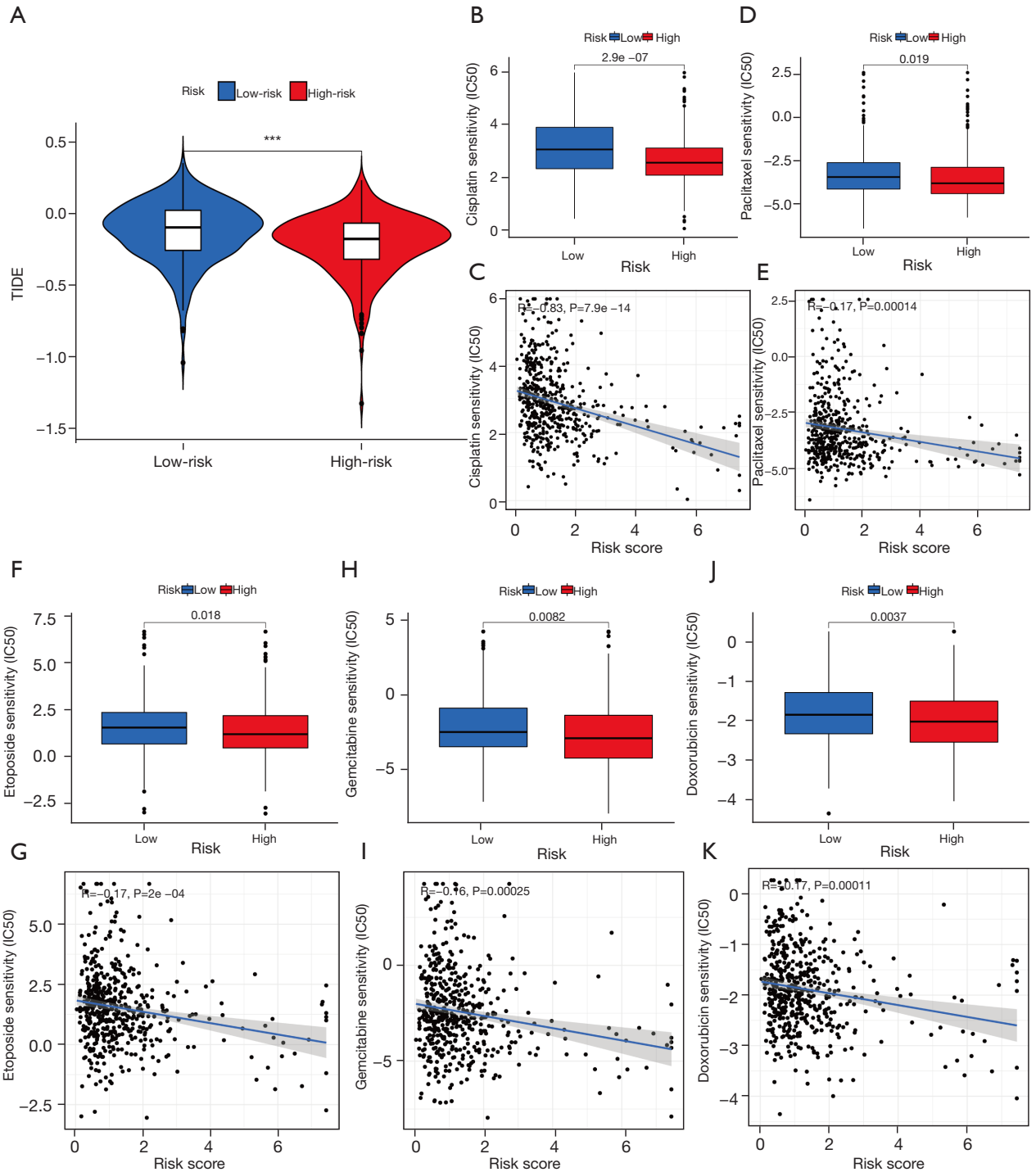

Figure 8 Sensitivity of immunotherapy and chemotherapy in LUAD patients. (A) Difference in TIDE score between low- and high-risk groups. (B-K) The correlation of risk score and the IC50 of (B,C) cisplatin, (D,E) paclitaxel, (F,G) etoposide, (H,I) gemcitabine, and (J,K) doxorubicin. TIDE was negatively correlated with immunotherapy sensitivity. TIDE, Tumor Immune Dysfunction and Exclusion; LUAD, lung adenocarcinoma; IC50, 50% inhibitory concentration, which was negatively correlated with drug responsiveness.

prognosis in LUAD (50,51). Dendritic cells and T follicular helper cells are considered to play important roles in anti-tumor immunity (51,52). In our study, we explored the association between the CLPS and TME heterogeneity in LUAD. DEGs between the high and low-risk groups were identified and demonstrated to be significantly enriched in biological pathways related to immune cell-infiltrating, ECM remodeling, and cytokine signaling. Combining results from the ESTIMATE and ssGSEA analyses, the high-risk group was characterized by a lower level of immune cell-infiltration (e.g., dendritic, B, $CD8^+$ T, and T helper cells) and immune activation. Moreover, significant negative correlations between the CLPS-risk score and the expression of immune checkpoint-related genes indirectly suggested the differences in the immunotherapeutic response rates of patients with different risk score (53). To further explore whether the CLPS could be used to predict the efficacy to immunotherapy, we evaluated differences in the TMB and TIDE score between high and low-risk groups. Cumulative evidence has indicated a higher TMB and lower TIDE were associated with a greater clinical response to immunotherapy (28,31). Significant differences in the TMB and TIDE score between the two groups demonstrated the ability of the CLPS to predict an immunotherapeutic response. Recent studies have revealed the interplay between immunotherapy and chemotherapy, and differences in immune infiltration have been shown to influence the resistance to adjuvant chemotherapy (54-56). In our results, patients with a higher CLPS-risk score exhibited better efficacy to five first-line chemotherapy drugs (including cisplatin, paclitaxel, etoposide, gemcitabine, and doxorubicin) in LUAD, suggesting additional potential of the CLPS to predict chemotherapy efficacy.

Despite the strengths and provocative observations as detailed above, our study had several limitations. First, there may be potential bias as the multivariate analysis was performed with limited clinical parameters available in a public dataset. Secondly, we could not directly analyze the association of cuproptosis-related lncRNAs and response to therapy due to the lack of detailed treatment information. Finally, the above findings were carried out mainly based on the bioinformatics analysis.

In conclusion, we successfully constructed a robust CLPS, which can potentially serve as a clinically effective tool to predict prognosis and predict response to immunotherapy and chemotherapy. Our findings also provide new insights into the role of cuproptosis in tumor progression and TME heterogeneity. CLPS contributes to further understand the regulatory mechanisms of cuproptosis on cancer development and offers a promising avenue for future targeted cancer therapy.

Acknowledgments

The authors would like to acknowledge the TCGA database for providing their platforms and those contributors for uploading their valuable datasets. The authors appreciate the academic support from the AME Lung Cancer Collaborative Group. The authors also appreciate the great support from Dr. Paul Toren (Centre de recherche sur le Cancer de l'Université Laval, Canada) in improving the quality of this paper.
Funding: None.

Footnote

Reporting Checklist: The authors have completed the TRIPOD reporting checklist. Available at https://tlcr.amegroups.com/article/view/10.21037/tlcr-22-660/rc

Conflicts of Interest: All authors have completed the ICMJE uniform disclosure form (available at https://tlcr.amegroups.com/article/view/10.21037/tlcr-22-660/coif). The authors have no conflicts of interest to declare.

Ethical Statement: The authors are accountable for all aspects of the work in ensuring that questions related to the accuracy or integrity of any part of the work are appropriately investigated and resolved. The study was conducted in accordance with the Declaration of Helsinki (as revised in 2013).

References

1. Sung H, Ferlay J, Siegel RL, et al. Global Cancer Statistics 2020: GLOBOCAN Estimates of Incidence and Mortality

Worldwide for 36 Cancers in 185 Countries. CA Cancer J Clin 2021;71:209-49.
2. Duma N, Santana-Davila R, Molina JR. Non-Small Cell Lung Cancer: Epidemiology, Screening, Diagnosis, and Treatment. Mayo Clin Proc 2019;94:1623-40.
3. Devarakonda S, Morgensztern D, Govindan R. Genomic alterations in lung adenocarcinoma. Lancet Oncol 2015;16:e342-51.
4. Miller KD, Nogueira L, Mariotto AB, et al. Cancer treatment and survivorship statistics, 2019. CA Cancer J Clin 2019;69:363-85.
5. Hirsch FR, Scagliotti GV, Mulshine JL, et al. Lung cancer: current therapies and new targeted treatments. Lancet 2017;389:299-311.
6. Tang D, Chen X, Kroemer G. Cuproptosis: a copper-triggered modality of mitochondrial cell death. Cell Res 2022;32:417-8.
7. Tsvetkov P, Coy S, Petrova B, et al. Copper induces cell death by targeting lipoylated TCA cycle proteins. Science 2022;375:1254-61.
8. Wang Y, Zhang L, Zhou F. Cuproptosis: a new form of programmed cell death. Cell Mol Immunol 2022;19:867-8.
9. Carneiro BA, El-Deiry WS. Targeting apoptosis in cancer therapy. Nat Rev Clin Oncol 2020;17:395-417.
10. Tang R, Xu J, Zhang B, et al. Ferroptosis, necroptosis, and pyroptosis in anticancer immunity. J Hematol Oncol 2020;13:110.
11. Liang C, Zhang X, Yang M, et al. Recent Progress in Ferroptosis Inducers for Cancer Therapy. Adv Mater 2019;31:e1904197.
12. Chen S, Shen X. Long noncoding RNAs: functions and mechanisms in colon cancer. Mol Cancer 2020;19:167.
13. Wang M, Mao C, Ouyang L, et al. Long noncoding RNA LINC00336 inhibits ferroptosis in lung cancer by functioning as a competing endogenous RNA. Cell Death Differ 2019;26:2329-43.
14. Bhan A, Soleimani M, Mandal SS. Long Noncoding RNA and Cancer: A New Paradigm. Cancer Res 2017;77:3965-81.
15. Pan J, Fang S, Tian H, et al. lncRNA JPX/miR-33a-5p/Twist1 axis regulates tumorigenesis and metastasis of lung cancer by activating Wnt/β-catenin signaling. Mol Cancer 2020;19:9.
16. Qu S, Jiao Z, Lu G, et al. PD-L1 lncRNA splice isoform promotes lung adenocarcinoma progression via enhancing c-Myc activity. Genome Biol 2021;22:104.
17. Deng X, Xiong W, Jiang X, et al. LncRNA LINC00472 regulates cell stiffness and inhibits the migration and invasion of lung adenocarcinoma by binding to YBX1. Cell Death Dis 2020;11:945.
18. Han X, Jiang H, Qi J, et al. Novel lncRNA UPLA1 mediates tumorigenesis and prognosis in lung adenocarcinoma. Cell Death Dis 2020;11:999.
19. Kuhn M. Building Predictive Models in R Using the Caret Package. J Stat Softw 2008;28:1-26.
20. Cobine PA, Brady DC. Cuproptosis: Cellular and molecular mechanisms underlying copper-induced cell death. Mol Cell 2022;82:1786-7.
21. Tibshirani R. The lasso method for variable selection in the Cox model. Stat Med 1997;16:385-95.
22. Yoshihara K, Shahmoradgoli M, Martínez E, et al. Inferring tumour purity and stromal and immune cell admixture from expression data. Nat Commun 2013;4:2612.
23. Hänzelmann S, Castelo R, Guinney J. GSVA: gene set variation analysis for microarray and RNA-seq data. BMC Bioinformatics 2013;14:7.
24. Charoentong P, Finotello F, Angelova M, et al. Pan-cancer Immunogenomic Analyses Reveal Genotype-Immunophenotype Relationships and Predictors of Response to Checkpoint Blockade. Cell Rep 2017;18:248-62.
25. Barbie DA, Tamayo P, Boehm JS, et al. Systematic RNA interference reveals that oncogenic KRAS-driven cancers require TBK1. Nature 2009;462:108-12.
26. Rosenberg JE, Hoffman-Censits J, Powles T, et al. Atezolizumab in patients with locally advanced and metastatic urothelial carcinoma who have progressed following treatment with platinum-based chemotherapy: a single-arm, multicentre, phase 2 trial. Lancet 2016;387:1909-20.
27. Mariathasan S, Turley SJ, Nickles D, et al. TGFβ attenuates tumour response to PD-L1 blockade by contributing to exclusion of T cells. Nature 2018;554:544-8.
28. Jiang P, Gu S, Pan D, et al. Signatures of T cell dysfunction and exclusion predict cancer immunotherapy response. Nat Med 2018;24:1550-8.
29. Ettinger DS, Wood DE, Aisner DL, et al. NCCN Guidelines Insights: Non-Small Cell Lung Cancer, Version 2.2021. J Natl Compr Canc Netw 2021;19:254-66.
30. Mayakonda A, Lin DC, Assenov Y, et al. Maftools: efficient and comprehensive analysis of somatic variants in cancer. Genome Res 2018;28:1747-56.
31. Yarchoan M, Hopkins A, Jaffee EM. Tumor Mutational Burden and Response Rate to PD-1 Inhibition. N Engl J Med 2017;377:2500-1.
32. Ready N, Hellmann MD, Awad MM, et al. First-Line Nivolumab Plus Ipilimumab in Advanced Non-Small-

Cell Lung Cancer (CheckMate 568): Outcomes by Programmed Death Ligand 1 and Tumor Mutational Burden as Biomarkers. J Clin Oncol 2019;37:992-1000.
33. Campbell JD, Alexandrov A, Kim J, et al. Distinct patterns of somatic genome alterations in lung adenocarcinomas and squamous cell carcinomas. Nat Genet 2016;48:607-16.
34. Cancer Genome Atlas Research Network. Comprehensive molecular profiling of lung adenocarcinoma. Nature 2014;511:543-50.
35. Imyanitov EN, Iyevleva AG, Levchenko EV. Molecular testing and targeted therapy for non-small cell lung cancer: Current status and perspectives. Crit Rev Oncol Hematol 2021;157:103194.
36. Ortega-Franco A, Calvo V, Franco F, et al. Integrating immune checkpoint inhibitors and targeted therapies in the treatment of early stage non-small cell lung cancer: a narrative review. Transl Lung Cancer Res 2020;9:2656-73.
37. Koren E, Fuchs Y. Modes of Regulated Cell Death in Cancer. Cancer Discov 2021;11:245-65.
38. Müller S, Raulefs S, Bruns P, et al. Next-generation sequencing reveals novel differentially regulated mRNAs, lncRNAs, miRNAs, sdRNAs and a piRNA in pancreatic cancer. Mol Cancer 2015;14:94. Erratum in: Mol Cancer 2015;14:144.
39. Yun MR, Lim SM, Kim SK, et al. Enhancer Remodeling and MicroRNA Alterations Are Associated with Acquired Resistance to ALK Inhibitors. Cancer Res 2018;78:3350-62.
40. Zhao K, Cheng J, Chen B, et al. Circulating microRNA-34 family low expression correlates with poor prognosis in patients with non-small cell lung cancer. J Thorac Dis 2017;9:3735-46.
41. Yu X, Zhang Y. Identification of a long non-coding RNA signature for predicting prognosis and biomarkers in lung adenocarcinoma. Oncol Lett 2020;19:2793-800.
42. Zhou YX, Zhao W, Mao LW, et al. Long non-coding RNA NIFK-AS1 inhibits M2 polarization of macrophages in endometrial cancer through targeting miR-146a. Int J Biochem Cell Biol 2018;104:25-33.
43. Lu Y, Luo X, Wang Q, et al. A Novel Necroptosis-Related lncRNA Signature Predicts the Prognosis of Lung Adenocarcinoma. Front Genet 2022;13:862741.
44. Li X, Pan X, Zhou H, et al. Comprehensive characterization genetic regulation and chromatin landscape of enhancer-associated long non-coding RNAs and their implication in human cancer. Brief Bioinform 2022;23:bbab401.
45. Liu Z, Mi M, Li X, et al. A lncRNA prognostic signature associated with immune infiltration and tumour mutation burden in breast cancer. J Cell Mol Med 2020;24:12444-56.
46. Pietras K, Ostman A. Hallmarks of cancer: interactions with the tumor stroma. Exp Cell Res 2010;316:1324-31.
47. Quail DF, Joyce JA. Microenvironmental regulation of tumor progression and metastasis. Nat Med 2013;19:1423-37.
48. Remark R, Becker C, Gomez JE, et al. The non-small cell lung cancer immune contexture. A major determinant of tumor characteristics and patient outcome. Am J Respir Crit Care Med 2015;191:377-90.
49. Altorki NK, Markowitz GJ, Gao D, et al. The lung microenvironment: an important regulator of tumour growth and metastasis. Nat Rev Cancer 2019;19:9-31.
50. Kudo M, Finn RS, Qin S, et al. Lenvatinib versus sorafenib in first-line treatment of patients with unresectable hepatocellular carcinoma: a randomised phase 3 non-inferiority trial. Lancet 2018;391:1163-73.
51. Cui C, Wang J, Fagerberg E, et al. Neoantigen-driven B cell and CD4 T follicular helper cell collaboration promotes anti-tumor CD8 T cell responses. Cell 2021;184:6101-6118.e13.
52. Palucka K, Banchereau J. Cancer immunotherapy via dendritic cells. Nat Rev Cancer 2012;12:265-77.
53. Hellmann MD, Nathanson T, Rizvi H, et al. Genomic Features of Response to Combination Immunotherapy in Patients with Advanced Non-Small-Cell Lung Cancer. Cancer Cell 2018;33:843-852.e4.
54. Wang W, Kryczek I, Dostál L, et al. Effector T Cells Abrogate Stroma-Mediated Chemoresistance in Ovarian Cancer. Cell 2016;165:1092-105.
55. Fu H, Zhu Y, Wang Y, et al. Identification and Validation of Stromal Immunotype Predict Survival and Benefit from Adjuvant Chemotherapy in Patients with Muscle-Invasive Bladder Cancer. Clin Cancer Res 2018;24:3069-78.
56. Zhu S, Zhang T, Zheng L, et al. Combination strategies to maximize the benefits of cancer immunotherapy. J Hematol Oncol 2021;14:156.

(English Language Editor: B. Draper)

Cite this article as: Ma S, Zhu J, Wang M, Zhu J, Wang W, Xiong Y, Jiang R, Seetharamu N, Abrão FC, Puthamohan VM, Liu L, Jiang T. A cuproptosis-related long non-coding RNA signature to predict the prognosis and immune microenvironment characterization for lung adenocarcinoma. Transl Lung Cancer Res 2022;11(10):2079-2093. doi: 10.21037/tlcr-22-660

